Shuffle-glide dislocation transformation in Si

Z. Li and R. C. Picu[a)]
Department of Mechanical, Aerospace and Nuclear Engineering, Rensselaer Polytechnic Institute, Troy, New York 12180, USA

(Received 13 December 2012; accepted 13 February 2013; published online 27 February 2013)

The transformation of dislocation cores from the shuffle to the glide set of {111} glide planes in Si is examined in this work. The transformation is thermally activated and is favored by a resolved shear stress which applies no force on the original perfect shuffle dislocation. A resolved shear stress driving dislocation motion in the glide plane is not observed to promote the transition. The stress-dependent activation energy for the described shuffle-glide transformation mechanism is evaluated using a statistical analysis. It is observed that the transformation is not associated with an intermediate metastable state, as has been previously suggested in the literature. © *2013 American Institute of Physics*. [http://dx.doi.org/10.1063/1.4793635]

I. INTRODUCTION

Silicon has a covalently bonded diamond cubic crystal with glide planes of {111} type. The {111} stacking involves two types of planes: the glide and the shuffle sets. These are shown schematically in a {110}-projection in Fig. 1. The interplanar spacing of the shuffle set (2.35 Å) is larger than that of the glide set (0.78 Å), but the bond density across the glide set is higher than that across the shuffle set by a factor of three. This observation suggests that the motion of dislocations is different in the two planes and this should have consequences on the mechanics of the crystal.

In macroscopic experiments, it is observed that Si is brittle at low temperatures and becomes ductile above 873 K—the temperature of the brittle-to-ductile transition.[1] This transition is produced in part by changes of the mobility of dislocations with temperature, and is intimately related to the contribution of the two types of glide planes to plasticity.

The competition between shuffle and glide systems has received significant attention over the past several decades,[2–8] in part due to the attempt to understand dislocation nucleation and motion in Si devices. It was concluded that a crystal deformed at low temperatures and large stresses deforms primarily by the motion of shuffle dislocations. At high temperatures and lower stress, mostly dislocations nucleating and moving in the glide plane cause plasticity.

Dislocation cores in the shuffle plane are undissociated, while those on the glide plane dissociate in partials. This can be explained based on the structure of the γ-surface corresponding to the two types of planes. The glide-set γ-surface has a minimum at the $\frac{1}{2}\langle 112\rangle$ position of the usual partial in face centered cubic crystals, while the shuffle-set γ-surface has no such minimum. Despite significant advances in the direct observation of core structures,[9,10] electron microscopy cannot distinguish directly between the shuffle and the glide sets, and the observation of dissociation usually indicates that the respective defect is located on the glide-set. In line with the above, at low temperatures dislocations are generally observed to be un-dissociated, while at high temperatures the situation is largely reversed.

Atomistic studies have shown that dislocations nucleate differently in the two sets. Shima *et al.*[11] calculated the activation energy for dislocation nucleation from a sharp 90° corner on the surface of Si as a function of the applied resolved shear stress. A full dislocation was considered when investigating the shuffle-set, while the nucleation of a partial was considered for the glide-set. It was observed that the curves representing the activation energy versus the applied stress intersect, which indicates that at low stresses nucleation in the glide set is favored. Interestingly, the activation energy for nucleation in the shuffle-set decreases with increasing pressure, while the activation energy corresponding to the glide-set is insensitive to the stress acting normal to the glide plane.

Considering that experimental observations indicate a preponderance of glide dislocations at high temperatures, the question remains whether dislocations can switch from one plane set to the other as the temperature is modified across the brittle-to-ductile transition. This has been a puzzle for a number of years. Theoretically, the transition can happen by climb for edge components of dislocations, or cross-slip for screw segments. Attempting an experimental demonstration of this idea, Saka *et al.*[12] tested single crystals of Si under supersaturation of interstitials and performed TEM observations. They concluded that the pre-existing shuffle set dislocations transformed to glide-set dislocations with dissociated cores, at about 400 °C. It should be noticed that these transitions are only observed at sharp bends of the dislocations. Dislocation climb was postulated to be the main mechanism controlling this physics. Under equilibrium concentration of vacancies, Justo *et al.*[13] observed no such transformation, further supporting the idea that climb controls shuffle-glide transitions. Another obvious mechanism leading to the same effect is the cross-slip of screw segments. This was postulated in Ref. 14, but was not directly observed in experiments. Rabier and Demenet[15] used TEM to examine the nucleation and migration of shuffle- and glide-set dislocations under different

a)Author to whom correspondence should be addressed. Electronic mail: picuc@rpi.edu.

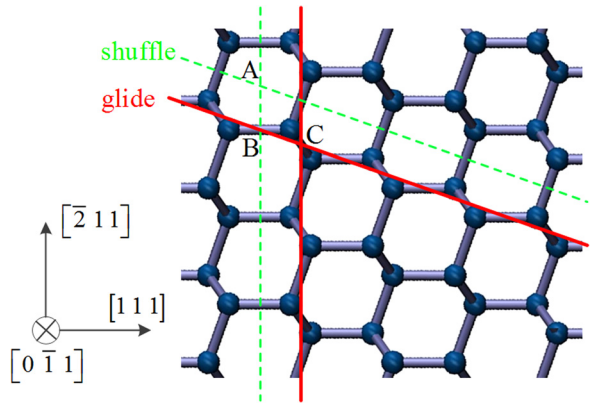

FIG. 1. {110} projection of the perfect Si lattice. The lines indicate {111} planes, with shuffle and glide planes shown with green dashed and red continuous lines, respectively. A, B, and C are three possible locations of the core.

loading conditions and did not uphold the possibility of dislocation core transformation.

A closer look at the potential mechanism of the shuffle-glide transformation, and focusing on screw segments, indicates that, before transformation, the shuffle core can be located at 3 types of positions denoted by A, B, and C (Fig. 1). The A and C cores are located at the intersection of two shuffle-set and two glide-set planes, respectively, while the B core lies at the intersection of a shuffle-set with a glide-set plane. It was found by density functional theory (DFT) and molecular dynamics (MD) simulations[16,17] that the B core has higher energy than the A and C cores. As a result, it can be assumed that the transformation from shuffle to glide requires overcoming a barrier before dissociation in the glide plane can happen.[16] Pizzagalli and Beauchamp[18] used first principle calculations to study the transition at 0 K and noted that the A to C transformation is not observed in their models. Guenole *et al.*[19] performed calculations combining the nudged elastic band method (NEB) and empirical potentials and obtained an activation energy ranging from 2.3 to 2.5 eV, function of the potential used. They concluded that the barrier is too high for the formation of the C core from A to be probable.

In this work, we study the shuffle to glide transition for screw dislocation segments at different temperatures and applied stresses. We consider stress states which do and do not produce a net driving force on the perfect, undissociated dislocation and show that the transition is favored by a stress with no shear component in the direction of the Burgers vector. The stress-dependent activation energy is evaluated. A resolved shear stress is not observed to lead to the transition rather its effect is to simply move the dislocation in the respective plane. The model and simulation methodology are presented in Sec. II, the phenomenology observed in simulations is discussed in Sec. III A, followed by the evaluation of the activation energy in Sec. III B. In Sec. III C, we discuss another phenomenon which takes over at very large stresses.

II. MODEL AND SIMULATION METHODOLOGY

Silicon is represented in these simulations using the three-body Stillinger-Weber (SW) potential,[20] which was used extensively in atomistic simulations of Si crystal mechanics. Given the technological importance of this material, a large number of potentials have been developed for Si, the most broadly used being SW, Tersoff,[21,22] and EDIP (Environment-dependent interatomic potential).[23] These potentials perform differently in different situations, each having its strengths and weaknesses. The SW potential is known to represent properly the energetics of reconstruction in the core of 30° partials in the glide plane, but to fail to represent the reconstruction predicted by *ab initio* models for the core of 90° glide partials.[23] The Tersoff potential fails to predict the reconstruction of the 30° partial. The newer EDIP potential appears to perform better with respect to the energetics of core reconstruction of both partials. An early comparison of many potentials, including SW and Tersoff is performed by Balamane *et al.*[24] The comparison performed in the EDIP article[23] leads to the conclusions mentioned above. In a more recent work, Godet *et al.*[25] compared these three potentials against *ab initio* data (DFT-local density approximation, DFT-LDA) specifically with respect to their performance with respect to large shear strains applied in the shuffle and glide {111} planes. This analysis is most relevant for the ability of potentials to represent dislocations. They conclude that the SW potential better reproduces the *ab initio* results with respect to the smoothness and the amplitude of the energy variation, as well as the localization of shear in the shuffle set. The SW potential provides the best approximation of the maximum restoring force for the ⟨110⟩ direction in the shuffle plane and the ⟨112⟩ direction in the glide plane, and for the theoretical shear strength and the strain associated with this critical stress in both planes. The un-relaxed unstable stacking fault energy for traces in the Burgers vector direction is best predicted for the ⟨110⟩ direction in the shuffle plane by the SW potential, and for the ⟨112⟩ direction of the glide plane by the EDIP potential. The values of the relaxed unstable stacking fault energy are best predicted by the Tersoff potential in both these crystal directions. In what concerns the proper representation of the motion of dislocations and the Peierls stress, the unstable stacking fault energy is less important than the rebound force of the lattice subjected to large deformations. Based on these results we infer that the SW potential is best suited to represent, at a minimum, undissociated shuffle dislocations and 30° partials in the glide plane, which are of main concern in this article.

The system is advanced in time using standard molecular dynamics and its parallel implementation in the LAMMPS package.[26] Let us consider the model shown in Fig. 2. The 3D simulation box has dimensions of $42 \times 42 \times 42\ a_0^3$, where $a_0 = 5.43$ Å is the lattice parameter of Si. The model contains 604 800 atoms. The crystal orientation is indicated in the figure, with GP1 and GP2 being two {111}-type glide planes (either of shuffle or glide type). A dipole of perfect screw dislocations with Burgers' vector $[01\bar{1}]$ is placed in the shuffle set of GP1 by displacing the atoms according to the anisotropic Volterra-Stroh solution. Initially, both dislocations are straight, with the dislocation lines lying along the $[01\bar{1}]$ direction. Periodic boundary conditions are used in all directions. Note that the model is large enough such that the periodic boundary conditions in the direction parallel to the dislocation line do not force the dislocations to remain straight during the simulation.

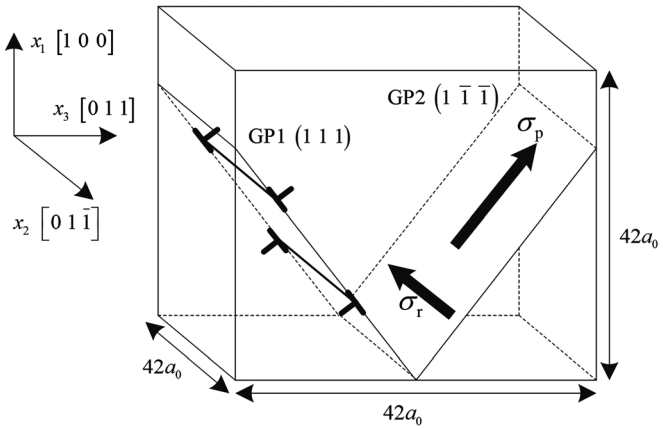

FIG. 2. Schematic representation of the model used, with two of the far field loadings shown. The two dislocations are of screw type. Therefore, σ_r produces a Peach-Koehler force, while σ_p does not.

The two dislocations forming the dipole attract each other. In order to have proper control on the applied stress, we eliminate the effect of the interaction by applying along the boundary of the model a uniform far field stress state producing exclusively a resolved shear stress which leads to a Peach-Koehler force that exactly balances that due to the interaction. Let us denote this stress by σ_0. The far field is applied in the form of imposed displacements which are computed using the anisotropic elastic stiffness tensor corresponding to the SW potential.

Two other types of far field stress are additionally considered (Fig. 2): a far field resolved shear stress, σ_r, which may move the two dislocations in plane GP2, and a far field stress with a shear component in the direction perpendicular to the Burgers vector in plane GP2, σ_p. This second field does not drive dislocation motion in any glide plane, while the first should promote cross-slip and dislocation motion in GP2. These states are applied in separate simulations, i.e., in given simulation the far field stress is either $\sigma_0 + \sigma_p$ or $\sigma_0 + \sigma_r$. Note that this is a schematic notation since σ_0, σ_r, and σ_p stand for entire stress tensors. In the discussion below, a numerical value specified for these parameters refers to the shear stress resolved in the direction of the Burgers vector in GP2 (in the case of σ_r) or the shear stress acting perpendicular to the Burgers vector in GP2 (in the case of σ_p), which are the only physically relevant quantities here.

As mentioned in the Introduction, a stress applied normal to the glide plane influences the nucleation and possibly the mobility of shuffle dislocations.[11] It has been also noted that this type of stress modifies the stacking fault and the unstable stacking fault energies for the shuffle plane while having only a marginal influence on these quantities corresponding to the glide plane.[27] Therefore, the mobility of shuffle dislocations depends on the normal stress on the glide plane. In order to avoid this effect, a hydrostatic stress is added to remove the normal stress.

III. RESULTS

A. The shuffle to glide transformation

To study the shuffle-glide transition, we consider first the stress state $\sigma_0 + \sigma_r$. Under this stress, and provided the driving σ_r is larger than the (temperature-dependent) Peierls stress, it was observed that the dislocation moves in GP2 while remaining in the shuffle plane. This conclusion holds for all temperatures studied, in the range 1 to 1500 K. In experiments, it is observed that glide-set dislocations predominate at high temperatures and low stresses and one would expect that as the temperature increases the transition to the glide-set should take place. Our observation suggests that simply increasing the temperature does not lead to the shuffle-glide transition under this type of stress.

When the stress state $\sigma_0 + \sigma_p$ is applied, the results are more interesting. At low temperatures, the dislocation remains un-dissociated and in the shuffle plane as long as $\sigma_p < 5$ GPa. Above approximately 1000 K, the dislocation shifts to the glide set of planes of GP2 and dissociates. The signature of a thermally activated process is observed: The process is stochastic and the transition happens with higher probability when the temperature and σ_p increase. In terms of the general phenomenology, this is in line with experimental observations and previous computational studies, while also indicating that the transition is driven by a non-resolved shear stress component.

Let us analyze the transition in more detail. Figure 3 shows a view of the glide plane GP2. The yellow line shows the position of the initial shuffle screw dislocation core. The several snapshots shown in Figs. 3(a)–3(c) are obtained from a molecular dynamics run in which dissociation was observed, at T = 1200 K and $\sigma_p = 3.4$ GPa. The red lines mark the location of the cores of two 30° partials belonging to the same glide-set plane. Denoting the partials as 30° is based on the orientation of their Burgers vector relative to the $[0\bar{1}1]$ direction of the initial screw dislocation. The partials nucleate from the original shuffle screw and spread sidewise in the glide-set. The green lines demarcate the un-dissociated and dissociated regions of the original screw dislocation. The region between the partials is a staking fault located in the glide-set of GP2.

The partials exhibit reconstructed configurations with successive rings containing 5 and 8 atoms. These reconstructed configurations, shown in Fig. 3(d), have been recognized as the ground-state of the 30° partial dislocations in the glide-set plane.[28] It has been found that the reconstruction of the dislocation core reduces the core energy by 0.36 eV/A.[8,29] The partials move by the propagation of kinks, as can be seen in Fig. 3.

Figure 4 shows a close-up view of the region marked by the continuous green line in Fig. 3(b) where the perfect screw dislocation residing in the shuffle-set decomposes in two partials located in the glide-set. The crystal is shown in the [011] projection. The region on the left of the image corresponds to the un-dissociated screw core, while that on the right represents the dissociated domain. Comparing the core structures observed here with those published in Refs. 19 and 28 and considered representative for specific planes, we confirm that the un-dissociated screw resides in the shuffle plane, while the dissociated partials are located in the glide set. This was further confirmed by measuring the interatomic planar shift in successive glide and shuffle planes parallel to GP2. Multiple sets of such snapshots resulting from simulations performed at other temperatures and applied

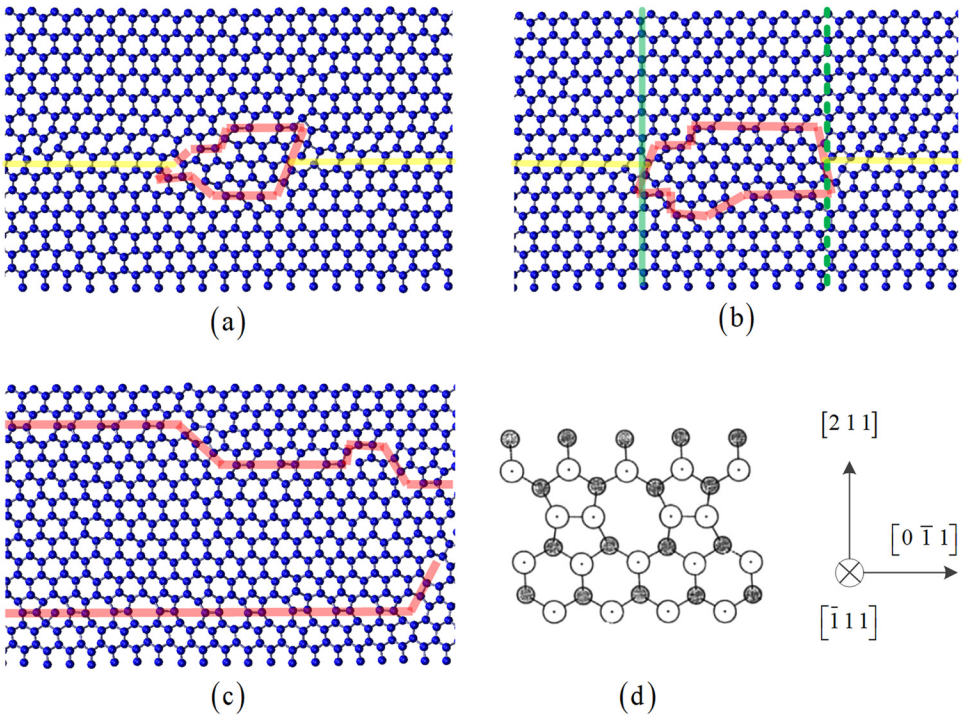

FIG. 3. (a)-(c) Snapshots representing intermediate atomic structures of the glide plane during the core transformation process. The dislocation lines for the 30° partials located in the glide set are indicated by the red lines. The initial position of the undissociated shuffle-set screw dislocation is indicated by the yellow line. The green lines in (b) indicate the boundary between dissociated and undissociated regions of the shuffle screw. (d) Ideal (reconstructed) core structure of the 30° partial located on the glide-set plane.[28] The coordinate system refers to all figures (a-d).

stresses were also analyzed and similar conclusions were drawn. It is also observed that the transition is abrupt, with no intermediate state being present between the shuffle and the glide-set segments of the dislocation. The transition takes place over a distance smaller than a_0 along the dislocation line, the core shifting from one atomic plane to the next.

These observations are important. They indicate that the shuffle to glide transformation does not involve an intermediate state as suggested in the literature.[19] Also, the transformation can be regarded as a nucleation process of the partial dipole located in the glide-set from a material defect, which is the shuffle screw dislocation in this case. The stress σ_p, acting perpendicular to the direction of the initial screw dislocation line and in GP2, leads to a Peach-Koehler force acting on the edge components of the two resulting partials, therefore favoring the dissociation. Since partials with edge components may exist only in the glide-set, it results that σ_p acts as an effective driving force for the transition. This substantiates the claim made above that the shuffle to glide transition is favored by a stress state which does not produce a Peach-Koehler force on the original screw dislocation.

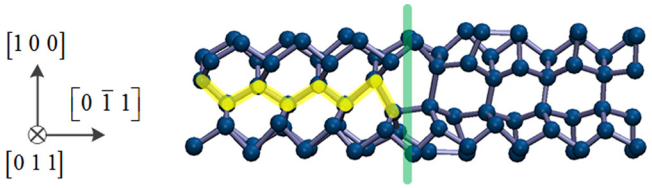

FIG. 4. Ball-stick representation of the undissociated shuffle screw–dissociated glide partials interface in the (011) projection. The green line indicates the interface of the dissociated and undissociated regions and corresponds to the continuous green line in Fig. 3(b). The undissociated screw dislocation lies on the left side of the green line, while the dissociated partials are on the right side. The core of the undissociated screw dislocation is indicated with the yellow line.

B. Evaluation of the activation energy

Since the transition bears the signature of a thermally activated process, we performed a statistical analysis aimed at estimating the stress-dependent activation energy. To this end, let us consider that the Arrhenius formulation holds, and compute the occurrence rate of a transformation event as

$$\dot{n}(\sigma_{sl}, T) = N\nu_0 \exp\left(-\frac{E(\sigma_p)}{k_B T}\right), \tag{1}$$

where n is the number of events observed, N is the number of sites where a transformation may take place, ν_0 is the attempt frequency, $E(\sigma_p)$ is the activation energy, and $k_B T$ is the energy of the thermal bath. $M = N\nu_0$ is the attempt rate, while n is the number of successful attempts. The activation energy is usually considered stress-dependent. The cumulative fraction function F(t, σ_p, T) can be related to the transformation rate $\dot{n}$ by considering that the time derivative of the cumulative fraction function $\dot{F}(t, \sigma_p, T)$ is proportional to the number of the transformation free replicas and to the transformation rate

$$\dot{F}(t, \sigma_p, T) = [1 - F(t, \sigma_p, T)] \cdot \dot{n}(\sigma_p, T). \tag{2}$$

By integrating this equation and substituting $\dot{n}$ from Eq. (1), the expression of the cumulative fraction function can be obtained as

$$\exp\left(-N\nu_0 t \exp\left(-\frac{E(\sigma_p)}{k_B T}\right)\right) = 1 - F(t, \sigma_p, T). \tag{3}$$

The activation energy results from (3) as

$$E(\sigma_p) = k_B T\{\log(N\nu_0 t) - \log[-\log(1 - F(t, \sigma_p, T))]\}. \tag{4}$$

The quantity F results directly from the simulations, $t = t_0 = 50$ ps is kept constant in all simulations, N represents

the number of sites along the initial screw dislocation at which the transformation may take place, ν_0 is the vibration frequency for the specific crystal. The value of N can be predicted from the nucleation properties, lattice type, and the size of the simulation box; the value of ν_0 can be assumed to be equal to the Debye frequency.[30] However, for better accuracy, we perform MD simulations at various temperatures and stress levels and determine the cumulative fraction F for each condition. The cumulative function is estimated from at least $M = 90$ replicas of given set of conditions.

Let us rearrange Eq. (4) as

$$T\log[-\log(1-F(t_0,\sigma_p,T))] = T\log(N\nu_0 t_0) - \frac{E(\sigma_p)}{k_B}, \quad (5)$$

set the applied stress at $\sigma_p = 2.9$ GPa, and consider situations with T = 1150, 1200, 1250, and 1300 K. The estimate for finite M of the left side of Eq. (5), $A = T\log[-\log(1-F(t_0,\sigma_p,T)]$, results from the simulations. This quantity is plotted in Fig. 5 versus T and the line represents the best fit to the data. The slope represents $\log(N\nu_0 t_0)$. The error bars are estimated by considering the process to be Poisson, with the probability of having n events out of M trials being $P(n,M) = e^{-\bar{F}M}(\bar{F}M)^n/n!$, with $\bar{F}$ being the large M limit of F. Then, the variance of n results $\langle(n-\bar{F}M)^2\rangle = \sum_{n'=0}^{\infty}(n'-\bar{F}M)^2P(n',M) = \bar{F}M$. We estimate $\bar{F}$ as the asymptote to which F converges in the limit of large M and then compute the standard deviation of F (shown in Fig. 5) as $\sqrt{\bar{F}/M}$. The data align reasonably well, which provides support for the use of the Arrhenius function of Eq. (1). From the slope, and with $t_0 = 50$ ps, we estimate $N\nu_0$ to be 1.97×10^6 GHz. This value is in the expected range since for Si the Debye frequency is 2×10^4 GHz and the number of possible nucleation sites along the dislocation line, N, is on the order of 100. We note that if the distribution function of A is Poisson, fitting the mean values in Fig. 5 is equivalent to fitting the entire distributions of A at all four values of the temperature. Disregarding this fact, the range of the slope of lines that can be drawn within the error bars in Fig. 5 is ±30% around the slope of the line fitted to the means (and shown in the figure).

To determine the stress dependence of the activation energy, simulations were performed at T = 1200 K and with $\sigma_p = 2.7$, 2.9, 3.1, 3.4, 3.7, and 3.9 GPa. Equation (4) is used to estimate $E(\sigma_p)$, with F computed by considering at least $M = 100$ replicas for each stress state. Figure 6 shows the results. The activation energy varies linearly with the applied stress, $E(\sigma_p) = E_0 - \sigma_p V$, where E_0 is the activation energy at zero stress and V is the activation volume. Fitting the data leads to $E_0 = 1.97$ eV and activation volume $V = 0.67|\mathbf{b}|^3$. The small value of V is related to the observation that the transition from shuffle to glide is a localized process, as discussed in Sec. III A and shown in Fig. 4. No intermediate state was observed, rather, the screw dislocation shifts directly from the shuffle to the glide plane under the action of the applied stress.

The activation energy for the mechanism proposed here is ~15% smaller than that associated with the mechanism discussed in Ref. 18 involving a transition from the A to the C core structure.

C. The large stress limit

Although less relevant for applications, it is worth noting another phenomenon which takes over at large values of σ_p. The process described in Sec. III A is controlled by the distortion of the core due to the applied shear stress σ_p. The distortion leads to the formation of an initially small edge dipole in the core of the screw dislocation, while the total edge component of the dislocation remains zero. The far field σ_p performs work on this dipole and, when its magnitude is large enough, leads to the formation of the two 30° partials, as described in Sec. III A. The interesting observation made in this context is that the partials shift to the glide-set of {111} planes, since partials may exist only in the glide-set.

When the stress increases, a transition is observed to the formation of full 60° dislocations instead of 30° partials. As

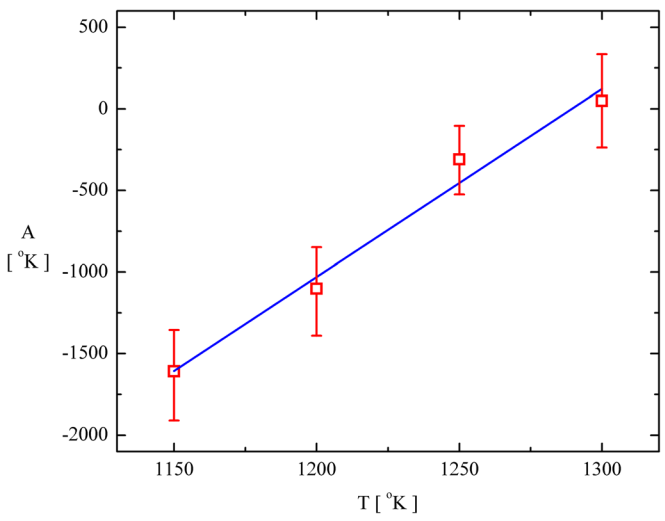

FIG. 5. Variation of the left side of Eq. (5), A, with the temperature. The line is the best fit to the data.

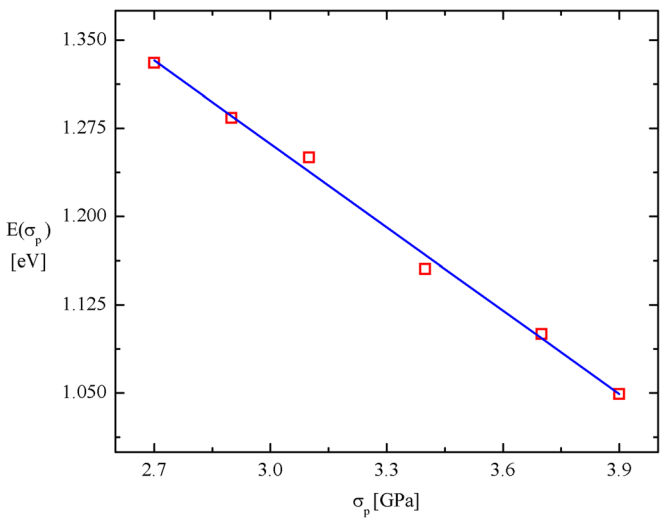

FIG. 6. Variation of the activation energy for the shuffle to glide transition of the screw dislocation with the applied stress σ_p. The squares indicate the values of $E(\sigma_p)$ obtained from Eq. (4). The line is the best fit to the data.

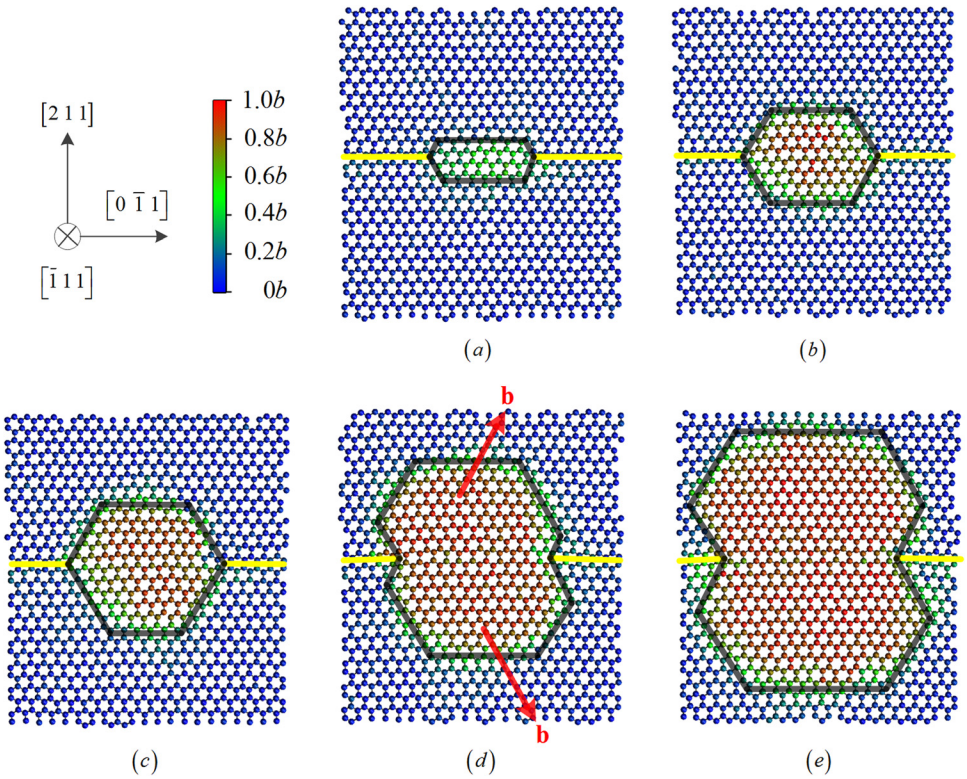

FIG. 7. Snapshots representing intermediate configurations of the shuffle-set of planes containing the initial screw dislocation (yellow straight line) and an un-dissociated 60° dislocation dipole nucleating from the screw. The colors represent the magnitude of the slip vector for each atom; b in the color bar equals 3.84 Å, representing the magnitude of the Burgers vector of a 60° dislocation.

before, denoting them as 60° dislocations is based on the orientation of their Burgers vector relative to the $[0\bar{1}1]$ direction of the initial screw dislocation. This is still a core effect and occurs once the work performed by σ_p is large enough to overcome the barrier associated with the nucleation of the two 60° full dislocations from the original screw dislocation. Obviously, the edge components of the Burgers vectors of the nucleated 60° dislocations have opposite sign such that their recombination leads to the original screw Burgers vector. Their magnitude is $\sqrt{6}/4a_0$, much larger than the magnitude of the edge component of the Burgers vector of the 30° partials, which is only $\sqrt{6}/12a_0$. The Schmid factor equals $\sqrt{3}/2$ for the 60° dislocations and 1/2 for the 30° partials. Importantly, the resulting dislocations remain in the shuffle plane and are not dissociated.

Figure 7 shows a series of snapshots of the shuffle plane GP2 with the position of the original screw dislocation marked by the straight yellow line. The simulation was performed at $T = 1200\,K$ and $\sigma_p = 5\,GPa$, i.e., a stress value above the range considered in Sec. III B. The position of the nucleating dislocations is marked by black lines. The color coding indicates the absolute value of the slip vector, which is the relative displacement of the atoms on the two sides of the shuffle plane. This relative displacement takes place in the direction of the Burgers vector which is shown in Fig. 7(d) for the two branches of the nucleating dislocations. The cores remain in the shuffle plane of GP2. It is also interesting to note the evolution of the slip vector during the initial stage of formation of the two 60° dislocations: A slip vector of length equal to that of the full Burgers vector appears only after the two nodes are separated by more than about $9a_0$ (compare the color within the loop in Figs. 7(a) to 7(c)). In the initial stages, a nucleus with a smaller slip vector increases in size and only once it reaches a critical size, the slip vector magnitude increases to the length of the Burgers vector.[31] The two nucleating half loops are of half-hexagonal shape which was also observed in other MD simulations[32] and in experiments performed at low temperature.[33]

This nucleation process is also thermally activated. The critical stress at which the 60° dipole nucleates decreases slightly as the temperature increases, but remains always significantly larger than the critical stress at which nucleation of the glide-set 30° partials is observed. This indicates that the energetic barrier for the nucleation of the shuffle-set dipole is larger than that discussed in Sec. III B. This barrier was not estimated since, given the large stresses involved, the importance of this phenomenon is obviously smaller than that of the shuffle-glide transition process.

IV. CONCLUSIONS

A mechanism of transformation of dislocations from the shuffle to the glide-set of planes in Si was described. It was shown that simple dislocation motion in the glide mode does not lead to the transition even as the temperature increases. The transition occurs when the core is distorted by a stress state which produces no Peach-Koehler force on the original shuffle dislocation. The distortion favors the formation of 30° partials which may exist only in the glide-set planes, and hence this stress drives the transition from the shuffle to the glide set. The process is thermally activated and the activation energy depends linearly on the applied stress. The zero-stress barrier height is estimated at 1.97 eV. As the stress distorting the core becomes larger, the process shifts to the nucleation from the original shuffle screw dislocation of a dipole of un-dissociated 60° full dislocations. The nucleated dipole resides

in the same shuffle-set plane as the initial screw. Core nonlinearities control both nucleation processes.

ACKNOWLEDGMENTS

This work was supported by IBM and the Center for Computational Nanotechnology Innovation (CCNI) at Rensselaer Polytechnic Institute.

[1]J. Samuels and S. G. Roberts, Proc. R. Soc. London, Ser. A **421**, 1 (1989), see http://www.jstor.org/stable/2398545.
[2]J. Rabier, P. Cordier, T. Tondellier, J. L. Demenet, and H. Garem, J. Phys.: Condens. Matter **12**, 10059 (2000).
[3]J. Godet, L. Pizzagalli, S. Brochard, and P. Beauchamp, Phys. Rev. B **70**, 054109 (2004).
[4]J. Godet, P. Hirel, S. Brochard, and L. Pizzagalli, J. Appl. Phys. **105**, 026104 (2009).
[5]I. L. F. Ray and D. J. H. Cockayne, Proc. R. Soc. London, Ser. A **325**, 543 (1971), see http://www.jstor.org/stable/77948.
[6]A. Gomez, D. J. H. Cockayne, P. B. Hirsch, and V. Vitek, Philos. Mag. **31**, 105 (1975).
[7]Q. Ren, B. Joós, and M. Duesbery, Phys. Rev. B **52**, 13223 (1995).
[8]M. S. Duesbery and B. Joos, Philos. Mag. Lett. **74**, 253 (1996).
[9]H. R. Kolar, J. C. H. Spence, and H. Alexander, Phys. Rev. Lett. **77**, 4031 (1996).
[10]J. C. H. Spence, H. R. Kolar, G. Hembree, C. J. Humphreys, J. Barnard, R. Datta, C. Koch, F. M. Ross, and J. F. Justo, Philos. Mag. **86**, 4781 (2006).
[11]K. Shima, S. Izumi, and S. Sakai, J. Appl. Phys. **108**, 063504 (2010).
[12]H. Saka, K. Yamamoto, S. Arai, and K. Kuroda, Philos. Mag. **86**, 4841 (2006).
[13]J. F. Justo, M. de Koning, W. Cai, and V. V. Bulatov, Phys. Rev. Lett. **84**, 2172 (2000).
[14]J. Rabier, J. L. Demenet, M. F. Denanot, and X. Milhet, Mater. Sci. Eng., A **400-401**, 97 (2005).
[15]J. Rabier and J. L. Demenet, Phys. Status Solidi A **202**, 944 (2005).
[16]A. Blumenau, R. Jones, T. Frauenheim, B. Willems, O. Lebedev, G. Van Tendeloo, D. Fisher, and P. Martineau, Phys. Rev. B **68**, 014115 (2003).
[17]L. Pizzagalli, P. Beauchamp, and J. Rabier, Philos. Mag. **83**, 1191 (2003).
[18]L. Pizzagalli and P. Beauchamp, Philos. Mag. Lett. **84**, 729 (2004).
[19]J. Guenole, J. Godet, and L. Pizzagalli, Modell. Simul. Mater. Sci. Eng. **18**, 065001 (2010).
[20]F. H. Stillinger and T. A. Weber, Phys. Rev. B **31**, 5262 (1985).
[21]J. Tersoff, Phys. Rev. B **37**, 6991 (1988).
[22]J. Tersoff, Phys. Rev. B **38**, 9902 (1988).
[23]M. Z. Bazant, E. Kaxiras, and J. F. Justo, Phys. Rev. B **56**, 8542 (1997).
[24]H. Balamane, T. Halicioglu, and W. A. Tiller, Phys. Rev. B **46**, 2250 (1992).
[25]J. Godet, L. Pizzagalli, S. Brochard, and P. Beauchamp, J. Phys.: Condens. Matter **15**, 6943 (2003).
[26]S. Plimpton, J. Comp. Phys. **117**, 1 (1995).
[27]L. Pizzagalli, J. L. Demenet, and J. Rabier, Phys. Rev. B **79**, 045203 (2009).
[28]V. V. Bulatov, S. Yip, and A. S. Argon, Philos. Mag. A **72**, 453 (1995).
[29]R. W. Nunes, Braz. J. Phys. **29**, 661 (1999).
[30]C. R. Weinberger, A. T. Jennings, K. Kang, and J. R. Greer, J. Mech. Phys. Solids **60**, 84 (2012).
[31]Z. Li, R. C. Picu, R. Muralidhar, and P. Oldiges, J. Appl. Phys. **112**, 034315 (2012).
[32]S. Izumi and S. Yip, J. Appl. Phys. **104**, 033513 (2008).
[33]J. Rabier and J. L. Demenet, Scr. Mater. **45**, 1259 (2001).